

Compressibility of Arterial Wall in Ring-cutting Experiments

K.Y. Volokh¹

Abstract: It is common practice in the arterial wall modeling to assume material incompressibility. This assumption is driven by the observation of the global volume preservation of the artery specimens in some mechanical loading experiments. The *global* volume preservation, however, does not necessarily imply the *local* volume preservation – incompressibility. In this work, we suggest to use the arterial ring-cutting experiments for the assessment of the local incompressibility assumption. The idea is to track the local stretches of the marked segments of the arterial ring after the stress-relieving cut. In the particular case of the rabbit thoracic artery, considered in this work, the following criteria for radial stretches come from preliminary analysis. If after the radial cut the marked segments shorten at the inner surface of the wall and lengthen at the outer surface while remaining unchanged in the middle of the wall then material is locally incompressible. If, however, the marked segments remain unchanged at the surfaces while lengthening in the middle of the wall then the material is locally compressible. Any other scenario would be an indication of the improper modeling assumptions, i.e. residual stresses are not relieved or material constants are inaccurate etc. It is believed that the proposed approach can be successfully implemented in experiments shedding new light on the arterial incompressibility issue.

keyword: Artery; Incompressibility; Hyperelasticity

1 Introduction

Incompressibility means preservation of a small material volume during deformation: $dv = dV$, where dV is a small volume around point \mathbf{X} before deformation and dv is the same volume around point \mathbf{x} after deformation $\mathbf{x} = \chi(\mathbf{X})$. Generally, the volume is not preserved: $dv = JdV$, where $J = \det \mathbf{F}$ and $\mathbf{F} = \text{Grad} \chi(\mathbf{X})$ is the deformation gradient. Thus, the incompressibil-

ity constraint can be formally written as $J = \det \mathbf{F} = 1 = \det \mathbf{F}^T \mathbf{F} = \det(2\mathbf{E} + \mathbf{1})$, where $\mathbf{E} = (\mathbf{F}^T \mathbf{F} - \mathbf{1})/2$ is the Green strain tensor and $\mathbf{1}$ is the identity tensor. Two points should not be missed. First, the definition of incompressibility is local, i.e. it should be obeyed at every point. The local incompressibility implies the global one. Indeed, we have in this case: $v = \int dv = \int dV = V$. The reverse is wrong: the global incompressibility does not imply the local incompressibility. Second, incompressibility is a geometric or kinematic constraint imposed on the deformation and it is not an intrinsic material property (all materials can be compressed to various degrees). Of course, some materials, e.g. water, show clear tendency to *isochoric* deformation obeying the incompressibility constraint. In this sense, they are called incompressible.

Why the notion of incompressibility is important? It is a matter of convenience. Analysis of mechanical behavior of materials can be significantly simplified with account of incompressibility. R.S. Rivlin mastered this approach giving elegant analytical solutions to numerous problems of nonlinear elasticity (Joseph and Barenblatt, 1997). The notion of incompressibility is also important for improving numerical algorithms of nonlinear finite element analysis (Bonet and Wood, 1997).

Are the arterial walls incompressible? This simple question has no simple answer. Experiments reported by Lawton (1954), Carew et al (1968), Dobrin and Rovick (1969), and Chuong and Fung (1984) suggest that "incompressibility holds at least globally" (Humphrey, 2002). This is natural that only global incompressibility can be observed in experiments. Any experiment deals with a finite specimen of artery. The conclusion about the local properties of the specimen is an extrapolation of the global observation. The validity of such extrapolation depends on the material under consideration. Many liquids, for example, are homogeneous, isotropic, and they do not resist shear stresses. Thus, the global stress/strain state can be highly homogeneous allowing for the conclusion that global incompressibility is a result

¹ On leave of absence from the Technion. Department of Mechanical Engineering, Johns Hopkins University, 3400 North Charles St, Baltimore, MD 21218 (E-mail: kvolokh@jhu.edu)

of the local one. This is not the case of arteries. They are anisotropic, inhomogeneous, compliant, and resist shear stresses. In the case of arteries, it is difficult to ensure a simple homogeneous stress/strain state, which could allow for drawing conclusions about the local incompressibility. Nonetheless, such conclusion is often made in desire to utilize the incompressibility constraint in calculations. Influenced by the seminal papers of Chuong and Fung (1983; 1984; 1986), the local incompressibility condition is widely used for material identification and assessment of residual stresses in arteries: Fung, 1984; Fung, 1990; Fung, 1993; Holzapfel and Ogden, 2003; Humphrey, 2002.

In this work, we suggest to use the arterial ring cutting experiments for the assessment of the local incompressibility assumption. The idea is to track the local stretches of the marked segments of the arterial ring after the stress-relieving cut. In the particular case of the rabbit thoracic artery, considered in this work, the following criteria for radial stretches come from preliminary analysis. If the marked segments shorten at the inner surface of the wall and lengthen at the outer surface while remaining unchanged in the middle of the wall then material is locally incompressible. If, however, the marked segments remain unchanged at the surfaces while lengthening in the middle of the wall then the material is locally compressible. Any other scenario would be an indication of the improper modeling assumptions, i.e. residual stresses are not relieved or material constants are inaccurate etc. It is believed that the proposed approach can be successfully implemented in experiments shedding new light on the arterial incompressibility issue.

2 Residual stresses and stretches in the arterial ring

In this section, we analyze the artery-cutting experiment with and without the incompressibility assumption. The results of this analysis are the theoretical basis for the proposal of the experiment, which will be considered in Discussion.

2.1 General background

Mechanical behavior of the arterial wall is prescribed analytically by a strain energy density per unit volume $W(\mathbf{E})$. In this case, the Cauchy stress is defined as follows

$$\boldsymbol{\sigma} = J^{-1} \mathbf{F} \frac{\partial W}{\partial \mathbf{E}} \mathbf{F}^T, \quad (1)$$

This stress obeys the following momentum balance law

$$\text{div} \boldsymbol{\sigma} = \mathbf{0}, \quad (2)$$

where body forces and inertia effects are ignored. Substituting Eq. (1) in Eq. (2) and adding boundary conditions

$$\begin{cases} \chi = \bar{\chi} & \text{on } \partial\Omega_\chi \\ \mathbf{t} = \bar{\mathbf{t}} & \text{on } \partial\Omega_{\mathbf{t}} \end{cases}, \quad (3)$$

it is possible to formulate a boundary value problem (BVP) of nonlinear elasticity. Here $\mathbf{t} = \boldsymbol{\sigma} \mathbf{n}$ is the surface traction; \mathbf{n} is a unit outward normal to body Ω in the current configuration; $\partial\Omega_\chi$ and $\partial\Omega_{\mathbf{t}}$ denote boundaries where placements and tractions are prescribed; barred quantities are given.

The formulation of BVP is slightly different when the geometric constraint of incompressibility is imposed. In this case, the strain energy function W should be extended enforcing the incompressibility condition with Lagrange multiplier² p

$$W^* = W(\mathbf{E}) + p(1 - \det(2\mathbf{E} + \mathbf{1}))/2. \quad (4)$$

Now, the stress is obtained by substituting W^* instead of W in Eq. (1)

$$\boldsymbol{\sigma} = -p\mathbf{1} + \mathbf{F} \frac{\partial W}{\partial \mathbf{E}} \mathbf{F}^T, \quad (5)$$

where the following result for invertible matrix \mathbf{A} has been used: $\partial(\det \mathbf{A})/\partial \mathbf{A} = \mathbf{A}^{-T} \det \mathbf{A}$ (Holzapfel, 2000). The new BVP described by Eqs. (2), (3), and (5) is incomplete because of the indeterminate Lagrange multiplier p . One scalar equation must be added, which is obtained from the condition:

$$\frac{\partial W^*}{\partial p} = \det(2\mathbf{E} + \mathbf{1}) - 1 = 0. \quad (6)$$

2.2 Arterial ring deformation

A typical problem, where the local incompressibility condition matters, is the assessment of residual stresses and stretches in arteries. To estimate the residual stress/strain state a ring excised from an artery is usually cut radially – Fig. 1. It is assumed that the opened segment is stress-free. The latter suggests considering the

²The Lagrange multiplier means hydrostatic pressure when the second term on the right hand side of Eq. (5) is deviatoric.

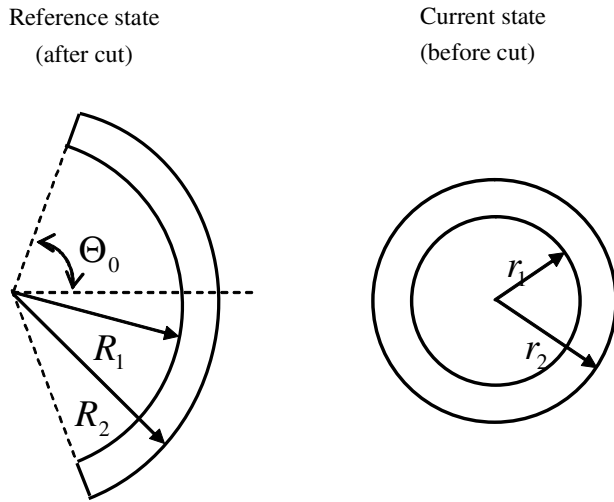


Figure 1 : Stress-relieving cut of the arterial ring.

opened ring as a reference configuration and the intact ring as the current one. The deformation can be described as follows

$$r = r(R), \quad \theta = \frac{\pi}{\Theta_0}\Theta, \quad z = \Lambda Z, \quad (7)$$

where (r, θ, z) are current cylindrical coordinates of the point with referential coordinates (R, Θ, Z) . It is assumed that deformation is axisymmetric and $\Theta_0 = \text{const}$ and $\Lambda = \text{const}$. In this case, the nonzero physical components of the deformation gradient tensor, i.e. stretches, and the Green strain tensor take the form

$$F_{rR} = \frac{\partial r}{\partial R}, \quad F_{\theta\Theta} = \frac{\pi r}{\Theta_0 R}, \quad F_{zZ} = \Lambda. \quad (8)$$

$$E_{RR} = \frac{1}{2} \left(\left(\frac{\partial r}{\partial R} \right)^2 - 1 \right), \quad E_{\Theta\Theta} = \frac{1}{2} \left(\left(\frac{\pi r}{\Theta_0 R} \right)^2 - 1 \right), \\ E_{ZZ} = \frac{1}{2} (\Lambda^2 - 1). \quad (9)$$

The deformation assumption given by Eq. (7) is quite reasonable in the case where the ring opens into a circular segment and most stresses are relieved by the cut.

2.3 Residual stresses and stretches with the incompressibility assumption

In this subsection, we reproduce³ analysis of Chuong and Fung (1986) starting with the incompressibility equation

$$J = \frac{\partial r}{\partial R} \frac{\pi r}{\Theta_0 R} \Lambda = 1, \quad (10)$$

which can be integrated analytically under condition $r(R_1) = r_1$

$$r^2 = \frac{\Theta_0}{\pi \Lambda} (R^2 - R_1^2) + r_1^2. \quad (11)$$

Substituting from Eqs. (10) and (11) in Eq. (9) it is possible to determine the strains completely.

Defining the strain energy density as follows

$$W = \frac{c}{2} e^Q, \\ Q = c_1 E_{RR}^2 + c_2 E_{\Theta\Theta}^2 + c_3 E_{ZZ}^2 + 2c_4 E_{RR} E_{\Theta\Theta} \\ + 2c_5 E_{ZZ} E_{\Theta\Theta} + 2c_6 E_{RR} E_{ZZ}, \quad (12)$$

we can compute nonzero components of Cauchy stress from Eq. (5)

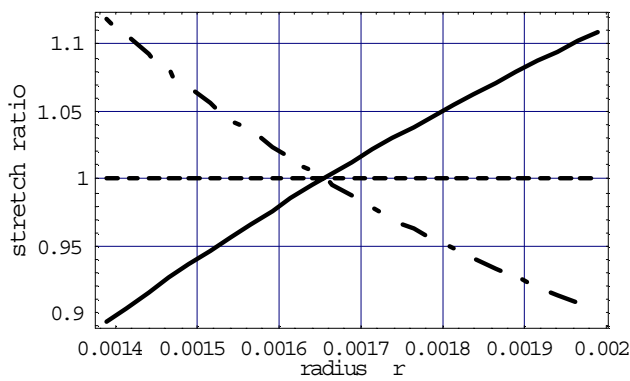
$$\begin{cases} \sigma_{rr} = -p + \left(\frac{\Theta_0 R}{\pi r \Lambda} \right)^2 c (c_1 E_{RR} + c_4 E_{\Theta\Theta} + c_6 E_{ZZ}) e^Q \\ \sigma_{\theta\theta} = -p + \left(\frac{\pi r}{\Theta_0 R} \right)^2 c (c_4 E_{RR} + c_2 E_{\Theta\Theta} + c_5 E_{ZZ}) e^Q \\ \sigma_{zz} = -p + \Lambda^2 c (c_6 E_{RR} + c_5 E_{\Theta\Theta} + c_3 E_{ZZ}) e^Q \end{cases} \quad (13)$$

It is still necessary to determine the Lagrange multiplier p . It can be done by integrating the only nontrivial equilibrium equation

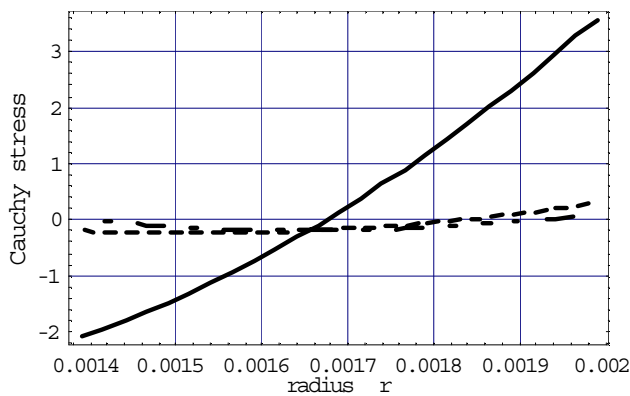
$$\frac{\partial \sigma_{rr}}{\partial r} + \frac{\sigma_{rr} - \sigma_{\theta\theta}}{r} = 0. \quad (14)$$

Substituting from (13) to (14) and integrating over r we find

$$p(r) = \left(\frac{\Theta_0 R}{\pi r \Lambda} \right)^2 c (c_1 E_{RR} + c_4 E_{\Theta\Theta} + c_6 E_{ZZ}) e^Q \\ + \int_{r_1}^r \left(\frac{\Theta_0 R}{\pi r \Lambda} \right)^2 c (c_1 E_{RR} + c_4 E_{\Theta\Theta} + c_6 E_{ZZ}) e^Q \frac{dr}{r} \\ - \int_{r_1}^r \left(\frac{\pi r}{\Theta_0 R} \right)^2 c (c_4 E_{RR} + c_2 E_{\Theta\Theta} + c_5 E_{ZZ}) e^Q \frac{dr}{r} \quad (15)$$

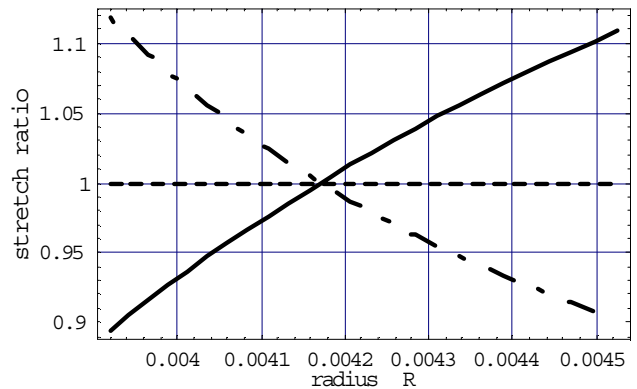


a.

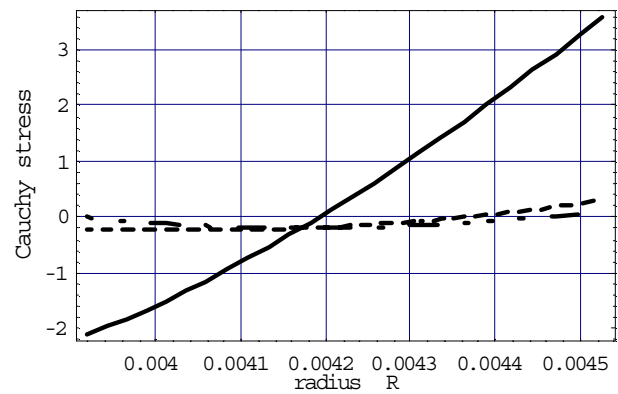


b.

Figure 2 : Stretches (a) and Cauchy (b) stresses with the incompressibility assumption (with respect to the current radial coordinate r). The point-dashed line for the radial quantities; the dashed line for the axial quantities; and the solid line for the circumferential quantities.



a.



b.

Figure 3 : Stretches (a) and Cauchy stresses (b) with the incompressibility assumption (with respect to the referential radial coordinate R). The point-dashed line for the radial quantities; the dashed line for the axial quantities; and the solid line for the circumferential quantities.

The integrals can be evaluated numerically after substituting for R from Eq. (11).

Following Chuong and Fung, we use the experimental data on a rabbit thoracic artery

$$\begin{aligned}
 R_1 &= 3.92 \text{ mm}, & R_2 &= 4.52 \text{ mm}, \\
 r_1 &= 1.39 \text{ mm}, & r_2 &= 1.99 \text{ mm}, \\
 \Theta_0 &= 71.4 \text{ deg}, & c &= 22.4 \text{ kPa},
 \end{aligned}
 \tag{16}$$

$$\begin{aligned}
 \Lambda &= 1, & c_1 &= 0.0499, & c_2 &= 1.0672, & c_3 &= 0.4775, \\
 c_4 &= 0.0042, & c_5 &= 0.0903, & c_6 &= 0.0585.
 \end{aligned}
 \tag{17}$$

Numerical integration has been performed with the help of Mathematica (Wolfram, 2003) and the resulting stresses and stretches are presented in Fig. 2 with respect to the current radial coordinate r . The results practically coincide with those obtained by Humphrey (2002) and are slightly different from the original results of Chuong and Fung (1986). Fig. 3 presents the same results with respect to the referential coordinate R , which will be used for the comparison purposes later in this work.

³Humphrey (2002) notes that the original results of Chuong and Fung are slightly inaccurate numerically.

2.4 Residual stresses and stretches without the incompressibility assumption

In this subsection, we relax the incompressibility assumption and we use the referential formulation of momentum balance

$$\text{Div} \mathbf{P} = \mathbf{0}, \quad (18)$$

or, in cylindrical coordinates (Volokh and Lev, 2005),

$$\begin{cases} \frac{\partial P_{rR}}{\partial R} - P_{\theta R} \frac{\partial \theta}{\partial R} + \frac{P_{rR}}{R} + \frac{\partial P_{r\Theta}}{R \partial \Theta} - \frac{P_{\theta \Theta}}{R} \frac{\partial \theta}{\partial \Theta} + \frac{\partial P_{rZ}}{\partial Z} - P_{\theta Z} \frac{\partial \theta}{\partial Z} = 0 \\ P_{rR} \frac{\partial \theta}{\partial R} + \frac{\partial P_{\theta R}}{\partial R} + \frac{P_{r\Theta}}{R} \frac{\partial \theta}{\partial \Theta} + \frac{P_{\theta R}}{R} + \frac{\partial P_{\theta \Theta}}{R \partial \Theta} + \frac{\partial P_{\theta Z}}{\partial Z} + P_{rZ} \frac{\partial \theta}{\partial Z} = 0 \\ \frac{\partial P_{zR}}{\partial R} + \frac{P_{zR}}{R} + \frac{\partial P_{z\Theta}}{R \partial \Theta} + \frac{\partial P_{zZ}}{\partial Z} = 0 \end{cases} \quad (19)$$

Here

$$\mathbf{P} = J \boldsymbol{\sigma} \mathbf{F}^{-T} = \mathbf{F} \frac{\partial W}{\partial \mathbf{E}} \quad (20)$$

is the 1st Piola-Kirchhoff stress tensor with the following nonzero components⁴

$$\begin{cases} P_{rR} = F_{rR} \frac{\partial W}{\partial E_{RR}} = \frac{\partial r}{\partial R} c(c_1 E_{RR} + c_4 E_{\Theta\Theta} + c_6 E_{ZZ}) e^Q \\ P_{\theta\Theta} = F_{\theta\Theta} \frac{\partial W}{\partial E_{\Theta\Theta}} = \frac{\pi r}{\Theta_0 R} c(c_4 E_{RR} + c_2 E_{\Theta\Theta} + c_5 E_{ZZ}) e^Q \\ P_{zZ} = F_{zZ} \frac{\partial W}{\partial E_{ZZ}} = \Lambda c(c_6 E_{RR} + c_5 E_{\Theta\Theta} + c_3 E_{ZZ}) e^Q \end{cases} \quad (21)$$

Eq. (19) reduces to the following form with account of axial symmetry and Eq. (8)

$$\frac{\partial P_{rR}}{\partial R} + \frac{P_{rR}}{R} - \frac{\pi P_{\theta\Theta}}{\Theta_0 R} = 0. \quad (22)$$

After substituting from Eqs. (9) and (21) in Eq. (22) and imposing stress-free boundary conditions

$$\begin{cases} \sigma_{rr}(R_1) = P_{rR}(R_1) = 0 \\ \sigma_{rr}(R_2) = P_{rR}(R_2) = 0 \end{cases} \quad (23)$$

we have a two-point boundary value problem in terms of $r(R)$. Its solution is obtained by using the shooting

method when the initial value problem (IVP) is solved iteratively until fitting the BVP solution. We used Mathematica (Wolfram, 2003) routine 'NDSolve' as the IVP solver. Cauchy stresses are obtained from Eq. (20) as follows

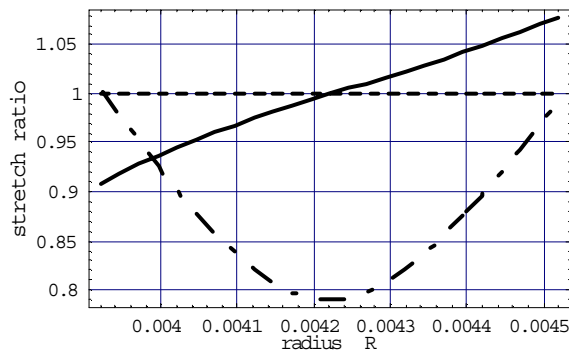
$$\begin{cases} \sigma_{rr} = J^{-1} F_{rR} P_{rR} \\ \sigma_{\theta\theta} = J^{-1} F_{\theta\Theta} P_{\theta\Theta} \\ \sigma_{zz} = J^{-1} F_{zZ} P_{zZ} \end{cases} \quad (24)$$

Stretches, stresses, and the volume ratio J computed from Eq. (22) with the input data given by Eqs. (16) and (17), are presented in Fig. 4. The radiuses of the intact ring were not included in the input but computed: $r_1 = r(R_1) = 1.41$ mm and $r_2 = r(R_2) = 1.93$ mm.

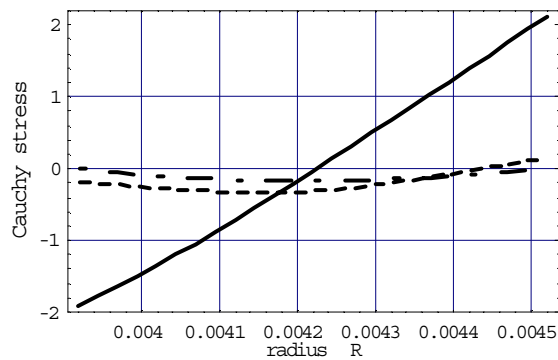
3 Discussion

The purpose of this work is to propose a possible experiment for examining the incompressibility property of arterial walls. The incompressibility assumption is often made for arteries based on some observations of the volume preservation of artery specimens. Such volume preservation, however, is usually a global property of the specimen under consideration. The volume preservation does not necessarily imply the local incompressibility, which is of interest only. Moreover, the global volume preservation may be a result of the specific experimental condition, i.e. it can be characteristic of the specific deformation under examination. To reveal the incompressibility property the experiments are necessary where the local incompressibility can be tracked at least qualitatively. The stress-relieving cut of the arterial ring is a good candidate for such an experiment. Analysis of the cut-ring opening has been performed with the incompressibility assumption, reproducing results of Chuong and Fung (1984) and Humphrey (2002), and without the incompressibility assumption. The distribution of stretches and stresses for both cases is given in Figs. 3a,b and 4a,b accordingly. It can be readily seen in figures 3b and 4b that stress distributions are quantitatively similar in both cases – with and without the incompressibility assumption, except for the hoop stresses at the outer surface of the ring where the enforcement of incompressibility leads to somewhat higher absolute magnitudes of the stresses. As follows from figures 3a and 4a the circumferential stretches are also similar whether the in-

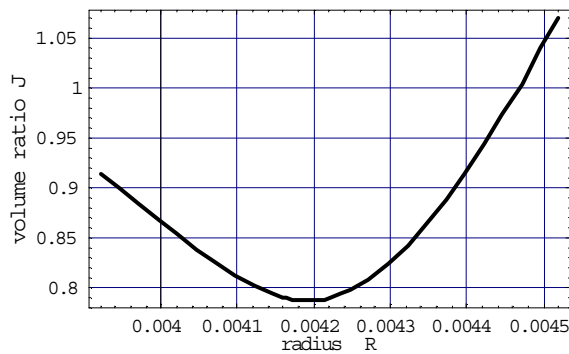
⁴ See Appendix



a.



b.



c.

Figure 4 : Stretches (a); Cauchy stresses (b); and volume ratios $J = \det \mathbf{F}$ without the incompressibility assumption (with respect to the referential radial coordinate R). The point-dashed line for the radial quantities; the dashed line for the axial quantities; and the solid line for the circumferential quantities.

compressibility assumption is accounted for or not. The axial stretches coincide as a direct consequence of the used deformation assumption given by Eq. (7). The only essential difference between two considered cases is the distribution of radial stretches. In the case of the incompressibility assumption, the radial stretches are computed from Eq. (6) and their graph is a mirror reflection of the distribution of circumferential stretches. In the case of compressibility, the radial stretches appear only after the solution of the corresponding boundary value problem and their distribution is not affected by the geometric restrictions. Evidently, the calculated distribution of the radial stretches does not meet the incompressibility requirement. The latter is emphasized in Fig. 4c where the volume ratio distribution is presented. The deviation from incompressibility is sensible in this case. Moreover, the global volume is not preserved.

It is very important for the experiment planning that the distinction between the radial stretches is not only quantitative, like in the case of hoop stresses, but also qualitative, what is crucial for a reliable experimental observation. This qualitative distinction suggests the radial stretches at the inner surface, in the middle, and at the outer surface of the ring to be observed in experiments. Let us assume that material fibers are marked in the mentioned areas of the intact ring. After the cut, the fibers will experience stretches opposite to those shown in figures (3) and (4). Particularly, the fibers will shorten at the inner surface and lengthen at the outer surface of the opened ring while remaining unchanged in the middle of the ring in the case where the deformation is incompressible. On the other hand, the fibers at the inner and outer surfaces of the opened ring will remain unchanged while the fibers in the middle of the ring will lengthen in the case where the deformation is compressible. If neither of these two scenarios takes place, the modeling assumptions are inapplicable and no definite conclusion about material behavior can be made.

References

- Bonet, J.; Wood, R.D.** (1997): *Nonlinear Continuum Mechanics for Finite Element Analysis*. Cambridge University Press, Cambridge.
- Carew, T.E.; Vaishnav, R.N.; Patel, D.J.** (1968): Compressibility of the arterial wall. *Circ Res.* vol. 23, pp. 61-68.

- Chuong, C.J.; Fung, Y.C.** (1983): Three-dimensional stress distribution in arteries. *J Biomech Eng.* vol. 105, pp. 268-274.
- Chuong, C.J.; Fung, Y.C.** (1984): Compressibility and constitutive relation of arterial wall in radial compression experiments. *J Biomech.* vol. 17, pp. 35-40.
- Chuong, C.J.; Fung, Y.C.** (1986): On residual stress in arteries. *J Biomech Eng.* vol. 108, pp. 189-192.
- Dobrin, P.B.; Rovick, A.A.** (1969): Influence of vascular smooth muscle on contractile mechanics and elasticity of arteries. *Am J Physiology.* vol. 217, pp. 1644-1651.
- Fung, Y.C.** (1984): *Biodynamics: Circulation.* Springer, New York.
- Fung, Y.C.** (1990): *Biomechanics: Motion, Flow, Stress, and Growth.* Springer, New York.
- Fung, Y.C.** (1993): *Biomechanics: Mechanical Properties of Living Tissues.* 2nd ed., Springer, New York.
- Holzapfel, G.A.** (2000): *Nonlinear Solid Mechanics: A Continuum Approach for Engineering.* John Wiley & Sons, Chichester.
- Holzapfel, G.A.; Ogden, R.W.** (2003): *Biomechanics of Soft Tissues in Cardiovascular Systems.* Springer, Wien.
- Humphrey, J.D.** (2002): *Cardiovascular Solid Mechanics: Cells, Tissues, and Organs.* Springer, New York.
- Joseph, D.D.; Barenblatt, G.I.** (1997): *Collected Papers of R.S. Rivlin.* Springer, New York.
- Lawton, R.W.** (1954): The thermoelastic behavior of isolated aortic strips of the dog. *Circ Res.* vol. 2, pp. 344-353.
- Volokh, K.Y.; Lev, Y.** (2005): Growth, anisotropy, and residual stresses in arteries. *MCB: Mechanics and Chemistry of Biosystems.* vol. 2, pp. 27-40.
- Wolfram, S.** (2003): *The Mathematica Book.* 5th edn, Wolfram Media.

Appendix A: On material constants

Computing material response with – Eq. (13) – and without – Eq. (21) – the incompressibility assumption, we use the same material constants $c, c_1, c_2, c_3, c_4, c_5, c_6$. It seems reasonable that material constants do not depend on the imposition or non-imposition of the geometric incompressibility constraint. To make this point clearer a reader may wish to consider the analogy between the in-

compressibility constraint and the geometric constraint imposed on thin elastic bodies – plates and shells. In the latter case, it is often assumed that the material fiber normal to the mid surface of the shell does not change its length and remains orthogonal to the mid surface during the deformation. These are the so-called Kirchhoff-Love geometric assumptions prompted by numerous physical observations. These assumptions-constraints are the driving forces for the development of the shell theories as an alternative to 3D elasticity. Although the Kirchhoff-Love assumptions are reasonable in many problems of shell deformation, they are not universal and can be accepted only when the shell thickness is much smaller than the length of the deformation half-wave. Evidently, the latter does not cover high-frequency vibrations, wave propagation, boundary effects etc. Let us assume now that we need to find the Young modulus (Poisson ratio is known) of an isotropic and homogeneous material of a thin plate. For this purpose, it is possible to bend the plate experimentally and to extract the Young modulus from the comparison of, say, the measured maximum deflection of the plate with its theoretical prediction. It is crucial, however, that the prediction can be made by using 3D elasticity without any geometric constraints or a plate theory where geometric constraints are enforced. Can the result of the Young modulus evaluation be different depending on what theory is used? The answer is, definitely, no. The situation with the incompressibility constraint for a compliant material seems to be analogous. The imposition of the constraint should not affect the determination of material constants.

We made this remark on the determination of material constants with and without the incompressibility assumption because Chuong and Fung (1984) stated that "the use of the incompressibility assumption greatly affects the material constants". Since this statement contradicts the remark given above, we revisit the results of Chuong and Fung, which gave rise to their statement.

A rectangular specimen of size $h \times a \times b$ excised from a rabbit thoracic aorta was placed by Chuong and Fung (1984) between two rigid plates. Nonzero pressure⁵ $\sigma_{11}(x_1 = \pm h/2) = \bar{\sigma}_{11}$ transmitted through the plates with no friction was measured while the specimen edges were stress-free $\sigma_{22}(x_2 = \pm a/2) = 0$ and $\sigma_{33}(x_3 = \pm b/2) = 0$. It was assumed that strains and stresses are

⁵The notation of the present work is adopted instead of the original notation of Chuong and Fung (1984).

homogeneous. Strains E_{11} , E_{22} , E_{33} were calculated after measuring the changing specimen size. Material constants were identified from the stresses, which obeyed boundary conditions and constitutive equations

$$\begin{cases} \sigma_{11} = -p + c(1 + 2E_{11})(c_1E_{11} + c_4E_{22} + c_6E_{33})e^Q \\ \sigma_{22} = -p + c(1 + 2E_{22})(c_4E_{11} + c_2E_{22} + c_5E_{33})e^Q \\ \sigma_{33} = -p + c(1 + 2E_{33})(c_6E_{11} + c_5E_{22} + c_3E_{33})e^Q \end{cases} \quad (25)$$

The measured deformation is incompressible ($J = 1$) and the enforcement of the incompressibility assumption in the constitutive equations is due to parameter p . Chuong and Fung describe two algorithms, with and without the incompressibility assumption, to identify 7 material constants c , c_1 , c_2 , c_3 , c_4 , c_5 , c_6 as follows. "For the incompressible case, subtraction of equations (A1₂) and (A1₃) from equation (A1₁) yields expressions of $\sigma_{11} - \sigma_{22}$ and $\sigma_{11} - \sigma_{33}$ in terms of the strain components with p cancelled. Seven sampling steps were carried out for each loading path, thus giving us fourteen simultaneous equations to solve. Without the incompressibility assumption, it is straightforward to solve 21 simultaneous equations. Numerically, the material constants are determined by minimizing the least-squares errors with the Gauss routine..." Performing numerical fit with two described algorithms, the authors obtained two essentially different sets of material constants, presented in Table 1 of the original paper, and they concluded, "...the use of the incompressibility assumption greatly affects the material constants". There is a point for discussion, however, in the authors' interpretation of the algorithms for fitting material constants.

First, let us assume that the incompressibility assumption is relaxed and equations (A1) do not include the Lagrange multiplier p . Then, instead of directly using the constitutive equations (A1) without p as Chuong and Fung suggest in their second algorithm, we subtract equations (A1₂) and (A1₃) from equation (A1₁) forming expressions of $\sigma_{11} - \sigma_{22}$ and $\sigma_{11} - \sigma_{33}$. This is legitimate, of course. Since the real deformation is isochoric ($J = 1$) then the expressions of the constitutive equations for the subtractions will be the same as the expressions of the constitutive equations for $\sigma_{11} - \sigma_{22}$ and $\sigma_{11} - \sigma_{33}$, which were obtained under the incompressibility assumption. This means that material constants

obtained by using the first Chuong and Fung algorithm with the incompressibility assumption are equally applicable to the case without the incompressibility assumption. Shortly speaking it is impossible to make a distinction between the enforced or relaxed incompressibility assumptions within the subtraction approach.

Second, let us assume that the material constants were obtained by the direct use of equation (A1) without p , as Chuong and Fung suggest in their second algorithm. The constitutive equations with these constants must obey the reduced constitutive equations for subtractions $\sigma_{11} - \sigma_{22}$ and $\sigma_{11} - \sigma_{33}$. The latter, however are equivalent to the constitutive equations with the enforced incompressibility assumption. In other words, the material constants obtained without the incompressibility assumptions must be the same as in the case where the incompressibility assumption was enforced. Again, no distinction between 'compressible' and 'incompressible' material constants can be made.

The fact that material constants calculated by Chuong and Fung have essentially different values should be attributed, in our opinion, to the numerical procedure, which minimizes the least-squares errors. There are some potential numerical pitfalls typical of the algorithms of this kind. These pitfalls cannot be analyzed with respect to the Chuong and Fung results because of the vital lack of the data in their report. Moreover, such analysis would bring us far beyond the scope of the present work.